УДК 54-161+544.653.22

https://doi.org/10.37827/ntsh.chem.2025.78.236

Khrystyna KHRUSHCHYK[1,2], Marta CHAVA[1], Veronika PIHEL[1], Julian KUBISZTAL[2], Vasyl KORDAN[1], Oksana HERTSYK[1], Malgorzata KAROLUS[2], Lidiya BOICHYSHYN[1]

CORROSION RESISTANCE OF THERMOMODIFIED AMORPHOUS ALLOY $Al_{87}Y_4Gd_1Ni_8$ IN THE TEMPERATURE RANGE 624-643 K

[1]*Ivan Franko National University of Lviv,*
Kyryla i Mefodiya Str., 6, Lviv 79005, Ukraine
e-mail: khrystyna.khrushchyk@us.edu.pl

[2]*University of Silesia in Katowice,*
Institute of Materials Engineering,
75 Pulku Piechoty, 1A, 41-500 Chorzow, Poland

In this work, the changes in the chemical composition of the surface of the amorphous metal alloy $Al_{87}Y_4Gd_1Ni_8$ as a result of isothermal annealing for two minutes in the air atmosphere at temperatures T_1 = 624±2, T_2 = 633±2, T_3 = 643±2 K, respectively, were studied by scanning electron microscopy. The annealing temperatures were determined from DSC (β=20 K/min) curves. The open circuit potentials were determined by the OCP method, which for this alloy are –0,618, –0,650, and –0,717 V, respectively. The following electrochemical parameters were determined by electrochemical impedance spectroscopy: the electrical equivalent elements used in the models are solution resistance (R_1), charge transfer resistance (R_3) and corrosion capacitor of the medium/corrosion products interface (CPE_{dl}), charge transfer resistance (R_3) in 0,3% aqueous NaCl solution.
It was found that with increasing annealing temperature, the values of solution resistance (R_1), passive film resistance (R_2), and charge transfer resistance (R_3), increase, indicating the formation of protective oxide layers on the surface of the alloys.
The influence of short-term annealing for 2 min in the temperature range of 624–643 K, which corresponds to the third stage of crystallisation, on the change in the electrochemical properties of the amorphous strip alloy $Al_{87}Y_4Gd_1Ni_8$ was investigated and the chemical composition of the amorphous metal alloys surface was found to change.

Keywords: amorphous metal alloys, aluminium, thermal modification, electrochemical parameters.

Introduction

Aluminium-based amorphous alloys (AMAs) are promising materials for the aerospace, automotive and electronics industries due to their low density combined with improved mechanical and corrosion properties compared to traditional crystalline aluminium alloys [1–10]. The homogeneous chemical composition and structure of the

amorphous state contribute to the formation of stable and passive oxide films on the surface, which effectively protect amorphous materials from aggressive environmental influences. However, the amorphous state is metastable and can undergo changes under the influence of heat treatment. Thermal modification, which is carried out to relax the structure or partially crystallise it, can significantly affect the physical and chemical properties of amorphous alloys, in particular, their corrosion resistance [4, 5, 8].

After heat treatment, when the temperature reaches the crystallisation point (T_c), phase transformations begin in the alloy, including the formation of nanocrystalline grains. This leads to a decrease in the corrosion potential due to the appearance of heterogeneous phases between which internal galvanic pairs can form and an increase in the corrosion current, as the newly formed grain boundaries and lattice defects become active zones of anodic dissolution. Also, partial nanocrystallisation can sometimes increase corrosion resistance due to the formation of a stable passive film. However, complete crystallisation tends to degrade electrochemical properties [10].

Therefore, electrochemical studies of corrosion processes occurring in aluminium-based AMAs after their thermal modification are important. The results of the study will allow us to expend the understanding of the corrosion properties of thermally modified aluminium AMAs and will contribute to the development of optimised heat treatment regimes to maintain or improve their corrosion resistance in practical applications.

Materials and methods of the experiment

Electrochemical studies of $Al_{87}Y_4Gd_1Ni_8$ AMAs in the form of a 20 mm wide and 35 μm thick strip, synthesized trans for study by the Institute of Metallophysics of the National Academy of Sciences of Ukraine, Kyiv, were carried out. Voltammetric studies of AMAs were carried out in the potentiodynamic mode using a PARstat 2273 (Revision 2273) potentiostat in the range of potentials set around the open circuit potential in an aqueous solution of 0.3% NaCl. A three-electrode cell was used: the working electrode (WE) was an amorphous alloy sample with an area of 0.5 cm², the reference electrode was a saturated calomel electrode (SCE, 0.242 V), and the counter electrode was a platinum plate. The obtained voltammetric curves were used to determine the main electrochemical parameters: corrosion potential (E_{corr}) and corrosion current density (j_{corr}), which reflect the degree of corrosion activity of the studied AMAs. The study was carried out by electrochemical impedance spectroscopy (EIS). The model of the equivalent circuit used to fit the EIS results is shown in Figure 1.

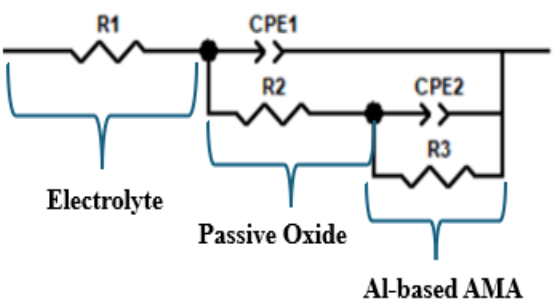

Fig. 1. Model of an equivalent circuit for fitting EIS results.

The electrical equivalent elements used in the model are: solution resistance (R_s), charge transfer resistance (R_{ct}) and corrosion medium/products interface capacitor (CPE_{dl}), charge transfer resistance (R_{ct}) being an important parameter and it is inversely proportional to the corrosion rate for each type of coating [6, 9]. Initial frequency: 20.0 kHz, final frequency: 10.0 mHz.

The $Al_{87}Y_4Gd_1Ni_8$ AMAs samples were modified by heat treatment for 2 minutes in air at temperatures of 624±2 K, 633±2 K, and 643±2 K, which were determined by DSC and selected according to the third stage of crystallisation.

Results and discussion

Annealing temperatures were determined from DSC curves. In these studies, the temperatures recorded at a heating rate (β) of 20 K/min were used.

To determine the change in the electrochemical parameters of AMAs in an aqueous solution of 0.3 % NaCl, the open circuit potential (OCP) method, which is a passive experiment, was used. In this mode, only the quiescent potential between the reference electrode and the working electrode is measured and is for $Al_{87}Y_4Gd_1Ni_8$ annealed at temperatures T_1 = 624±2 K, T_2 = 633±2 K, T_3 = 643±2 K.

The establishment of the equilibrium potential took 15 hours, which is five times longer compared to the initial AMAs of the same composition. Fig. 2 shows the last 15 minutes of the process of establishment of the equilibrium potential.

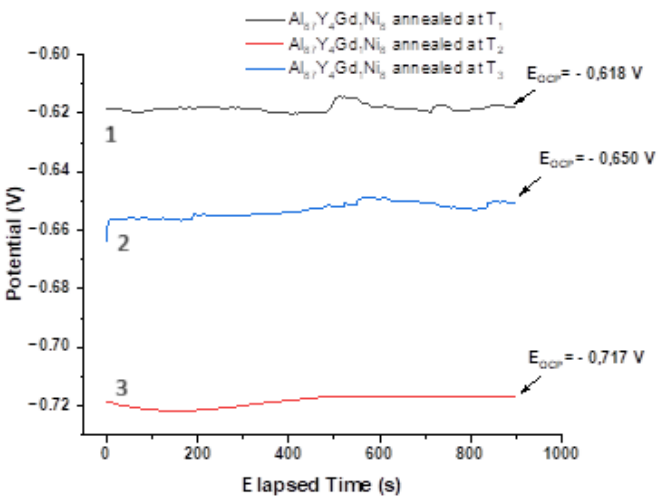

Fig. 2. Determination of the open circuit potential for $Al_{87}Y_4Gd_1Ni_8$ AMAs annealed at temperatures T_1 = 624± 2 K (1), T_2 = 633± 2 K (2), T_3 = 643± 2 K (3), respectively.

Using the equivalent circuit (Fig. 1), we determined the change in the electrochemical parameters of AMAs as a result of annealing (Fig. 3, Table 1). Figure 3 shows typical Nyquist curves and graphs of the change in the phase angle for $Al_{87}Y_4Gd_1Ni_8$ after heat treatment at temperatures T_1, T_2, T_3.

As can be seen from Table 1, the solution resistance (R1) and charge transfer resistances (R_3) increase with increasing annealing temperature. The constant phase

element (CPE) is treated as a pure resistor when n = 0, a pure capacitor when n = 1, and a Warburg impedance when n = 0.5. In this model, R_1, R_2, and R_3 are the solution resistance, passive film resistance, and charge transfer resistance in the double layer, respectively, while CPE1 and CPE2 represent the CPE to the passive film and double layer, respectively. Hence, this model assumes that the passive film is defective and should not be treated as a homogeneous layer.

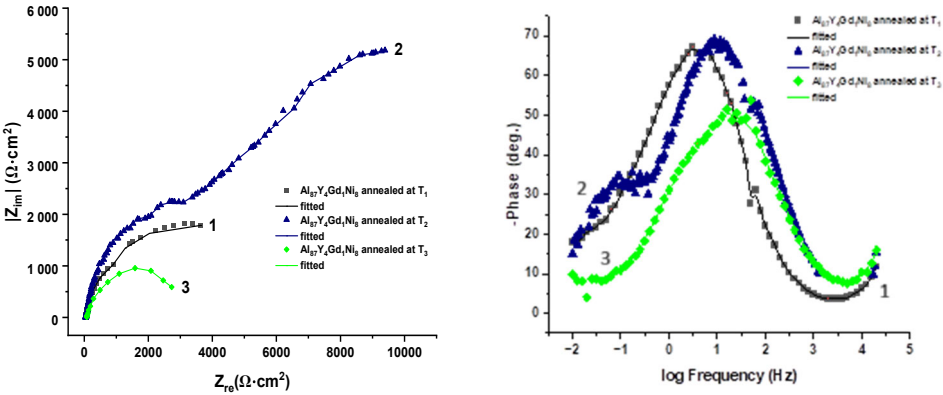

a *b*

Fig. 3. Experimental Nyquist diagrams (a) and phase angle plots (b) for $Al_{87}Y_4Gd_1Ni_8$ AMAs heat-treated sample at T_1 = 624±2 K (1), T_2 = 633±2 K (2), T_3 = 643±2 K (3).

Table 1

Electrochemical parameters obtained from the fitting of EIS results for $Al_{87}Y_4Gd_1Ni_8$ AMAs after heat treatment at temperatures T_1 = 624± 2 K, T_2 = 633± 2 K, T_3 = 643± 2 K

Annealing temperature ±2, K	R_1, Ω cm^2	R_2, Ω cm^2	CPE1 (Ω^{-1} cm^{-2}) ·10^{-5}	*n*	R_3, Ω·cm^2	CPE2 (Ω^{-1} cm^{-2}) ·10^{-3}	*n*
initial	45.600				4800.0	0.0450	0.8700
624	37.6(7)	324.0(1)	21.50(1)	0.85(7)	78(8)	3.40(5)	0.68(7)
633	211.0(6)	2.1(5)	1.21(3)	1.98(7)	2283(1)	3.36(5)	0.60(1)
643	78.6(5)	206.0(5)	6.40(2)	0.76(5)	9(9)1	0.20(1)	0.77(5)

A passive film can be described as a complex membrane structure consisting of various layers of insoluble oxide that protect the surface from corrosion. In some cases, the point resistance of an alloy is determined by the passive film formed on its surface. The Al_2O_3 oxide film is unstable in water. It usually transforms into AlOOH or $Al(OH)_3$, which is more stable than the Al_2O_3 film.

Further nanocrystallisation of the alloys, when nanocrystals of an already solid solution of Al(R) and intermetallic compounds are released (as a result of annealing at temperatures), on the contrary, shifts the corrosion potentials to the cathode region, activates pitting corrosion processes and leads to an increase in the corrosion current (Table 2). The surface layers are compacted, which improves the corrosion characteristics of AMAs, in particular, a significant expansion of passivation areas on the voltammogram.

Annealing at T_3 leads to the formation of a surface granular, possibly porous structure. Solution ions diffuse through the pores faster, thereby provoking corrosion, which is reflected in higher values of the corrosion current density.

It was found from the voltammetric curves that corrosion currents increase as a result of annealing, which indicates the intensification of corrosion processes on the surface of AMAs. However, the corrosion potentials shifted to the anodic side (Table 2) and the oxygen content of the AMAs surface increased (Fig. 4), which may indicate surface passivation and the formation of an oxide film.

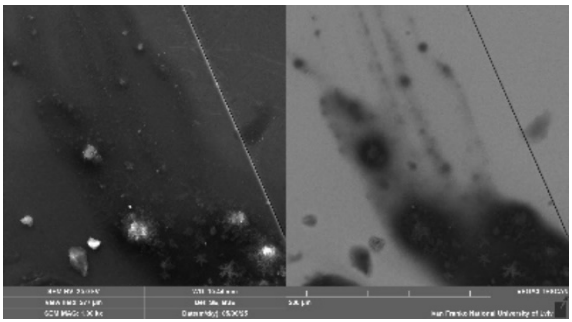

a

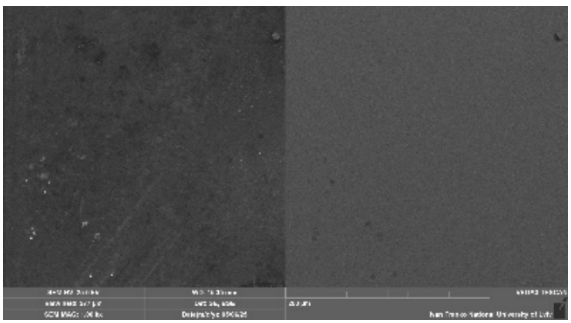

b

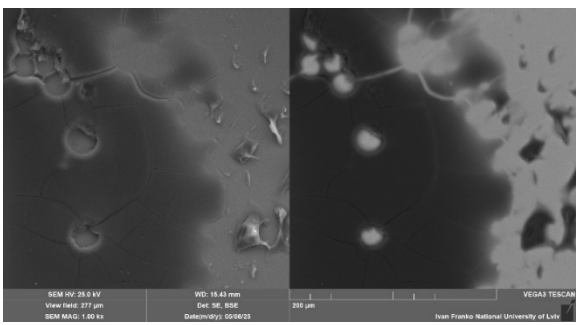

c

Fig. 4. Microphotographs of the AMAs surface after annealing at temperatures at (a) T_1= 624±2, (b) T_2= 633±2, (c) T_3=643±2 K. (magnification of 1000 times).

Table 2.

Main characteristics of corrosion in 0.3% NaCl solution. $Al_{87}Y_4Gd_1Ni_8$ AMAs after heat treatment

Annealing temperature ±2, K	-E_{corr}, V	j_{corr}, A/cm^2 ×10^8
initial state	0,61	1,31
633	0,62	2,69
643	0,54	51,2

The corrosion potentials shifted to the anodic side (Table 2) and the oxygen content of the AMAs surface increased (Fig. 4, Table 3), which may indicate surface passivation and the formation of an oxide film (Fig. 5).

Table 3.

Changes in the content of elements on the surface (at. %) of AMAs after annealing

Annealed temperatures ±2, K	Contain of the elements, at.%			
	Al	Y	Gd	Ni
624	85.94	4.69	0.96	8.42
633	86.56	3.72	0.92	8.80
643	83.39	5.85	1.15	9.61

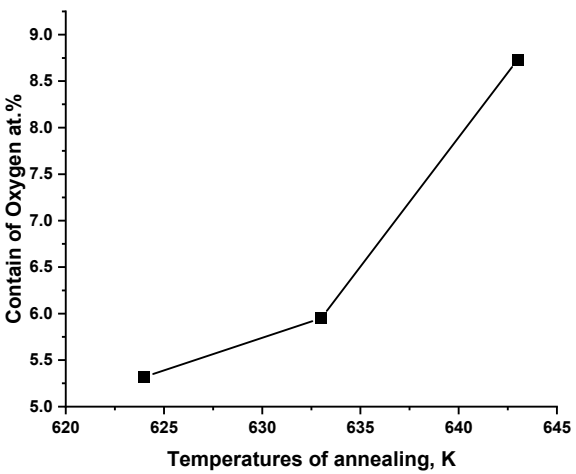

Fig. 5. Changes in the oxygen content on the surface of AMAs after annealing at temperatures T_1 = 624±2, T_2 = 633±2 and T_3 =643±2 K.

Conclusions

A short-term heat treatment of $Al_{87}Y_4Gd_1Ni_8$ strip AMAs was carried out at the temperatures of the third crystallisation stage at the temperatures of the third crystallisation stage.

It was found that with an increase in the annealing temperature, the values of solution resistance (R_1), passive film resistance (R_2), and charge transfer resistance (R_3) increase, indicating the formation of protective oxide layers on the surface of the alloys.

The open circuit potential (OCP) decreases with increasing heat treatment temperature, indicating a shift in electrochemical activity to the cathodic direction and the development of passivation processes. The passive film on the surface of the alloys is heterogeneous, has a multilayer structure and contains impurities of intermetallic phases and mixed oxides, which was confirmed by SEM and EDX analysis.

The heat treatment of the samples leads to changes in the surface morphology and distribution of alloying elements (Ni, Gd, Y), which significantly affects the corrosion resistance of the alloys. The most noticeable signs of pitting corrosion activation were found for the alloys after heat treatment at a maximum temperature of 643±2 K, that explains by increasing of corrosion current density (j_{corr}).

Acknowledgement

The results of the research were obtained with the financial support of the Ministry of Education and Science of Ukraine (state registration number of the state budget topic: 0123U101830 "Nanocrystallization of amorphous cobalt-based alloys: kinetics, properties, applications").

REFERENCES

1. *Louzguine-Luzgin D. V., Ketov S. V., Trifonov A. S., Churymov A. Yu.* Surface structure and properties of metallic glasses. J. Alloys Compd. 2018. Vol. 742. P. 512–517. https://doi.org/10.1016/j.jallcom.2018.01.290.
2. *Wang Z., Wang X., Xu C., Zhao Y., Qu X.* Hybrid nanostructured aluminum alloy with super-high strength. NPG Asia Materials. 2015. Vol. 7. P. 1–8. https://doi.org/10.1038/am.2015.129.
3. *Nizameiev M., Hertsyk O., Boichyshyn L.* Physicochemical properties of amorphous and nanocrystalline alloys: Structure, physical-mechanical and corrosion properties of amorphous and nanocrystalline iron-based alloys. – LAP Lambert Academic Publishing, 2022. – 292 p.
4. *Hertsyk O.M., Kovbuz M.O., Pereverzeva T.H., Borysyuk A.K., Boichyshyn L.M.* Influence of heat treatment and variable magnetic fields on the chemical resistance of amorphous alloys based on iron. Mater. Sci. 2014. Vol. 50(3). P. 454–460. https://doi.org/10.1007/s11003-014-9742-3.
5. *Ivanov Y.P., Meylan C.M., Panagiotopoulos N.T., Georgarakis K., Greer A.L.* In situ TEM study of the crystallization sequence in a gold-based metallic glass. Acta Materialia. 2020. Vol. 196. P. 52–60. https://doi.org/10.1016/j.actamat.2020.06.021
6. *Ma H., Cheng X., Li Y., Chen S.* Impedance investigation of the anodic iron dissolution in perchloric acid solution. Corrosion Science. 2002. Vol. 44(6). P. 1177–1191. https://doi.org/10.1016/S0010-938X(01)00145-7.
7. *Warski T., Kolano-Burian A., Garstka K., Nabialek M., Jeż B.* Influence of Cu content on structure and magnetic properties in $Fe_{86-x}Cu_xB_{14}$ alloys. Materials. 2020. Vol. 13. Article No. 1451. https://doi.org/10.3390/ma13061451.
8. *Lashgari H.R., Wang G., Xu J., Zhang Y., Zhang H.F., Li J.S.* Thermal stability, dynamic mechanical analysis and nanoindentation behavior of FeSiB(Cu) amorphous alloys. Materials Science and Engineering: A. 2015. Vol. 626. P. 480–499. https://doi.org/10.1016/j.msea. 2014.12.097.

9. *Lazanas A.Ch., Prodromidis M.I.* Electrochemical Impedance Spectroscopy A Tutorial. ACS Measurement Science Au. 2023. Vol. 3(3). P. 162–193. https://doi.org/10.1021/acsmeasuresciau.2c00070.
10. *Pajkossy T., Jurczakowski R.* Electrochemical impedance spectroscopy in interfacial studies. Current Opinion in Electrochemistry. 2017. Vol. 1(1). P. 53–58. https://doi.org/10.1016/j.coelec.2017.01.006.

РЕЗЮМЕ

Христина ХРУЩИК[1,2], Марта ЧАВА[1], Вероніка ПІГЕЛЬ[1], Юліан КУБІШТАЛЬ[2], Василь КОРДАН[1], Оксана ГЕРЦИК[1], Малгоджата КАРОЛУС[2], Лідія БОЙЧИШИН[1]

КОРОЗІЙНА СТІЙКІСТЬ ТЕРМОМОДИФІКОВАНОГО АМОРФНОГО СПЛАВУ $AL_{87}Y_4GD_1NI_8$ В ДІАПАЗОНІ ТЕМПЕРАТУР 624–643 К

[1]*Львівський національний університет ім. Івана Франка,*
вул. Кирила і Мефодія, 6, 79005 Львів, Україна
e-mail: khrystyna.khrushchyk@us.edu.pl

[2]*Сілезький університет в Катовіцах*
Інститут інженерії матеріалів,
вул. 75 Пулку Піхоти, 1, 41-500 Хожув, Польща

Аморфні сплави на основі алюмінію є перспективними матеріалами для аерокосмічної, автомобільної та електронної промисловості завдяки низькій густині у поєднанні з покращеними механічними та корозійними властивостями порівняно з традиційними кристалічними алюмінієвими сплавами. Однорідний хімічний склад і структура аморфного стану сприяють утворенню стабільних пасивних оксидних плівок на поверхні, які ефективно захищають аморфні матеріали від агресивного впливу навколишнього середовища. Тому електрохімічні дослідження корозійних процесів, що відбуваються в алюмінієвих АМА після їх термічної модифікації, є важливими. Результати дослідження дозволять нам розширити розуміння корозійних властивостей термічно модифікованих алюмінієвих АМА та сприятимуть розробці оптимізованих режимів термічної обробки для підтримки або покращення їхньої корозійної стійкості в практичному застосуванні.

За допомогою скануючої електронної мікроскопії досліджено зміни хімічного складу поверхні аморфного металевого сплаву $Al_{87}Y_4Gd_1Ni_8$ в результаті ізотермічного відпалу протягом двох хвилин в атмосфері повітря за температур T_1 = 624±2, T_2 = 633±2, T_3 = 643±2 К відповідно. Температури відпалу визначалися за кривими ДСК (β=20 К/хв).

Потенціали розімкнутого кола для цього сплаву становлять –0,618, –0,650 та –0,717 В, відповідно. Наступні електрохімічні параметри визначалися за допомогою електрохімічної імпедансної спектроскопії: електричними еквівалентними елементами, що використовуються в моделях, є опір розчину (R_1), опір переносу заряду (R_2) та корозійний конденсатор межі розділу середовище/продукти корозії (CPE), опір переносу заряду (R_3) у 0,3% водному розчині NaCl.

Встановлено, що зі збільшенням температури відпалу значення опору розчину (R_1), опору пасивної плівки (R_2) та опору переносу заряду (R_3) збільшуються, що вказує на утворення захисних оксидних шарів на поверхні сплавів.

Досліджено вплив короткотривалого відпалу протягом 2 хв в діапазоні температур 624–643 К, що відповідає третій стадії кристалізації, на зміну електрохімічних властивостей аморфного стрічкового сплаву $Al_{87}Y_4Gd_1Ni_8$ та виявлено зміну хімічного складу поверхні аморфних металевих сплавів.

Ключові слова: аморфні металеві сплави, алюміній, термічна модифікація, електрохімічні параметри.

Стаття надійшла: 15.07.2025.
Після доопрацювання: 20.08.2025.
Прийнята до друку: 26.09.2025.